IEEE Access
Multidisciplinary | Rapid Review | Open Access Journal

Received 5 January 2023, accepted 5 February 2023, date of publication 9 February 2023, date of current version 14 February 2023.

Digital Object Identifier 10.1109/ACCESS.2023.3243727

RESEARCH ARTICLE

Optimal Design of Modular Electrical Infrastructure for Large-Scale Electric Bus Depots

MINA ESKANDER, MAIK PLENZ, EDVARD AVDEVICIUS, AND DETLEF SCHULZ, (Senior Member, IEEE)
Department of Electrical Engineering, Helmut Schmidt University, 22043 Hamburg, Germany
Corresponding author: Mina Eskander (mina.eskander@hsu-hh.de)

This work was supported in part by the dtec.bw—Digitalization and Technology Research Center of the Bundeswehr (Digitalization and E-Mobility) under Grant UT 7001.

ABSTRACT Owing to the immense climate changes recently, the city of Hamburg has decided to allow the purchase of only emission-free buses for public transportation. Meanwhile, Hamburg focuses on the implementation of electric buses. For this purpose, the two public transportation companies in Hamburg which are the Hamburger Hochbahn AG (HOCHBAHN), and the Verkehrsbetriebe Hamburg-Holstein GmbH (VHH) decided to build new charging infrastructure for electric bus depots. In addition, they started by electrifying their existing stations. This study proposes an optimal method for electrifying bus depots by modularizing the subsystems in electrical power systems. An approach that allows the study of different configurations of power system components. Analyzing these configurations results in the conclusion of the most technically feasible configuration, achieving the lowest cost. Furthermore, the model objectives include reducing the required area, which is a challenging criterion for bus depots in many cities. Mixed-Integer Quadratic Programming (MIQP) is used to generate this combination based on predefined constraints that must satisfy all implemented constraints of the system.

INDEX TERMS Power system optimization, modularization of system components, electric bus depots, mixed-integer quadratic programming (MIQP).

NOMENCLATURE

C_{B}	The cost, which is created from blocked buses.
C_{Cable}	Sum of costs of cable components.
C_{cHV}	Sum of costs of all selected HV network cables.
C_{cTyp}	Sum of costs of all selected charger cables for buses.
C_{THV}	Sum of costs of all selected HV network transformers.
C_{Total}	Sum of costs of grid components.
$C_{\mathrm{Transformer}}$	Sum of costs of all transformer components.
C_{Typ}	Sum of costs of all selected bus transformers for buses.
CP_{ij}^{C}	Set of all considered cable prices following the line i -j.
$CP_{i'}^{\mathrm{T}}$	Set of all considered transformer prices at node i'.
h_j	Charging task at time instance j.
$H^{\max}$	Maximum number of buses charging at the same time.
$H(t)$	Power consumption as a function in time (t).
I_{ij}^{C}	Set of all considered cable nominal ampacities of the chosen cables following the line $i-j$.
L_{D}	Constant, which represents the length of the planned depot in meters which is defined by the user at the beginning of the simulation.
L_{F}	Constant, which represents the length of the free area that is planned to allow buses to leave the parking slot (space between carports).
L_{TCC}	Integer variable, which represents the total length of cables for lengths of carports.

The associate editor coordinating the review of this manuscript and approving it for publication was N. Prabaharan.

L_{TSC} Integer variable, which represents the total length of series carports of both bus types.

L_{Typ} Constant, which represents the length of a bus according to its type in meters.

L_{TypC} Integer variable, which represents the length of planned carport for buses.

L_{TypCC} Integer variable, which represents the total length of cables required for buses.

L_{TypF} Integer variable, which represents the total planned free area length for buses in meters.

L_{TypT} Integer variable, which represents the total lengths of buses in meters according to their configuration.

L_{TypTC} Integer variable, which represents total length of carports.

N_{ij}^{cCH} Integer variable describing how many 1 m-cables from each type following the line $i-j$ are selected for the chargers.

N_{CH} Integer variable, which represents the total number of chargers in the bus depot.

N_{ij}^{cHV} Integer variable describing how many 1 m-cables from each type following the line $i-j$ are selected for the high voltage network side.

N_{i}^{cTyp} Integer variable, deciding on the number of 1 m-cables to be used for the buses-network.

N_{FL} Integer variable, which represents the number of free area lengths (considering the area length as a variable to be optimized).

N_{FW} Integer variable, which represents the number of free area widths (considering the area width as a variable to be optimized).

N_{Limit} Constant, which can be predefined to vary the limitation in number of buses.

$N_{i'}^{\mathrm{sTHV}}$ Integer variable describing the total number selected from each type of transformer in the point of connection of the bus depot with the grid.

$N_{i'}^{\mathrm{sTyp}}$ Integer variable representing the total number of transformers for buses at node i'.

N_{TVTyp} Integer variable, which represents the selected number of transformers for each type of bus.

N_{Typ} Integer variable, which represents the total number of buses needed to serve all the routes of each type.

$N_{\mathrm{Typper\ C}}$ Integer variable, which represents the number of buses per carport.

N_{TypC} Integer variable, which represents the number of carports.

N_{TypCP} Integer variable, which represents the number of parallel carports for buses.

N_{TypCS} Integer variable, which represents the number of series carports for articulated buses.

N_{TypP} Integer variable, which represents the number of buses parking parallel to each other in a carport.

N_{TypS} Integer variable, which represents the number of buses parking in series in a carport.

P_{Ch} Charging power of the buses per charger.

P_{N} Peak power at the point of connection with the grid.

$P_{i'}^{\mathrm{T}}$ Set of all transformer power from the data base to be placed at node i'.

P_{THV} Continuous variable, which represents power consumption per transformer of the high voltage network.

P_{Typ} Continuous variable, which represents power consumption per transformer of the carports.

P_{TypC} Continuous variable, which represents power consumption per carport.

PF Power factor, which is defined as the ratio of working power to apparent power.

T_{C} Set of all considered cables.

T_{P} Set of all considered transformers.

T Set of simulated time of 24 hours.

UF Utilization factor in the bus depot, which ranges between 0 (no buses are charging at the same time) to 1 (all buses are charging the same time).

V_{ij}^{c} Set of the cable nominal voltages.

V_{LV} Low voltage at the charger which is predefined to be 0.4 kV (in case of having a medium voltage at the grid connection point of 10 kV or 20 kV, the $V_{i'}^{\mathrm{s}} = V_{\mathrm{LV}} = 0.4$ kV).

$V_{i'}^{\mathrm{p}}$ Set of possible primary voltage of the transformer at the grid point of connection (i'). It is determined based on the $V_{\mathrm{p,grid}}$.

$V_{\mathrm{p,grid}}$ Chosen high level voltage for the electrical network which is either 110 kV, 20 kV, or 10 kV depending on the peak power consumption of the depot.

$V_{i'}^{\mathrm{s}}$ Set of possible secondary voltage of the transformer at the grid point of connection (i'). It is also determined based on the cost.

V_{SHV} Integer variable representing the calculated secondary voltage of the transformer at the grid point of connection.

W_{D} Constant, which represents the width of the planned depot in meters which is defined by the user at the beginning of the simulation.

W_{F} Constant, which represents the width of the free area which is planned to allow buses to leave the parking slot (space between carports).

W_{TCC} Integer variable, which represents the total length of cables for widths of carports.

W_{TPC}	Integer variable, which represents the total width of parallel carports of both bus types.
W_{Typ}	Constant, which represents the width of a bus in meters.
$\theta_{ij}^{\mathrm{cCH}}$	Binary variable deciding on the types of cables from the set T_{C} to be used for the chargers.
$\theta_{ij}^{\mathrm{cHV}}$	Binary variable deciding on the types of cables from the set T_{C} used on the high voltage side following the line i -j.
$\theta_{ij}^{\mathrm{cTyp}}$	Binary variable deciding on the types of cables to be used for the buses-network.
$\theta_{i'}^{\mathrm{sTHV}}$	Binary variable deciding on the type of transformer from the set T_{P} is chosen to be used for the HV-network or not.
$\theta_{i'}^{\mathrm{sTyp}}$	Binary variable deciding on the types of transformers from the set T_{P} to be used for buses at node i'.
Π	Set of calculated nodes for chargers.
ψ	Set of calculated nodes for high voltage level.
Ω	Set of calculated nodes for buses.

I. INTRODUCTION

The importance of reducing the use of fossil fuels has recently gained more attention worldwide. Recent extreme climate changes have intensely emphasized this initiative. Involvement of the transportation sector plays an important role in this improvement [1]. Reducing the emissions from the public transportation segment represents significant progress towards a clean environment. One of the major challenges facing the use of electric buses is the charging infrastructure. This owes to the complexity of finding an optimum design that satisfies both cost and technical aspects without affecting the operation. However, it is easier to plan the electrification of buses infrastructure in comparison with other transportation ways as the routes are predefined in advance. Several studies have demonstrated the possibility of optimizing the Total Cost of Ownership (TCO) of bus depots as a function of the number of passengers [2]. Others consider optimization based on scheduling algorithms with a focus on opportunity charging and its difference from depot charging, but without considering construction costs [3]. The authors of [4] studied the optimum number of chargers along the routes for opportunity-charging models. Their target was to minimize the total cost of ownership by optimizing the location of chargers and the battery capacity per bus. In another prospective study, the authors of [5] analyzed the curtailment possibilities for a large-scale bus depot without affecting depot operation. They targeted the downsizing of the system components to reduce the infrastructure total costs. The authors of [6] studied the electrification of public transportation networks. They considered both opportunity and depot charging. Their research is based on categorizing depots into groups with different battery capacities. They showed that depot charging requires more buses to cover predefined routes. In [7], the authors presented a planning tool for bus depots that considered various technical and operational aspects. This tool enables the study of parking, vehicle dispatching and price-oriented charging. In [8], the authors assessed the effect of charging buses in depots on a grid. In their study, they considered the depot and opportunity charging. They observed a 30% increase in peak power demand in winter.

In [9], the authors focused on concluding cost-optimal feeding stations for a transportation network applied to an opportunity-charging model. In general, showing the optimum design of charging infrastructure motivates bus operators to electrify their depots. Subsequently, this decreases the impact of integrating electric vehicles into the distribution network [10]. The authors in [11] developed a MILP model, that can be used to optimize the design of electric mobility services for a Local Energy Community (LEC). Their focus was to combine microgrid with Photovoltaic (PV) plants and storage systems with the demand of electric shuttles and sharing vehicles. As a result, they concluded the optimum number of vehicles and charging stations associated with PV and storage systems considering their costs. Authors in [12] developed a placement approach for electric freight trucks, which serve in a Multi-Depot Multi-product distribution system. Their objective was to obtain the optimum location-routing for the trucks with regarding the supply distribution to realize the minimum system costs. In [13] a MILP model is presented to design and operate a distributed energy system optimally. Authors focused in their study on optimizing the heating, cooling and electricity loads for an urban neighborhood. In [14] a MILP model is developed to identify the energy storage system potential for one bus depot combined with three charging stations along the route. Their contribution was to design a battery storage system, that can mitigate the peak demands to reduce the electricity bills. In [15] a case study for solving an optimization problem of routing and charging electric vehicles is presented. The authors decomposed the MIP problem into two linear programming problems. In [16] a study of the optimal sizing and efficient routing for an electric vehicle-on-demand system is conducted. Authors developed a MILP model to satisfy the system requirements at minimum investment. Their objective was to reduce the total number of electric vehicles by scheduling a suitable assignment for them. The authors in [17] developed a MILP model for multistage planning of electric vehicle charging stations. Their objective was to identify the optimum size, location and installation time of system components. Furthermore, they planned the services of charging stations to cover electric vehicles users geographically at the minimum costs.

The estimation of the load profile is the first step in designing the charging infrastructure. Nevertheless, after determining the required capacity, the problem embraces optimizing the components needed in the bus depot. Based on the total profile, the transformer configurations could have been determined, only if all buses were placed in one carport. This optimization problem involves the dependency of the design

process on other factors, such as the arrangement of buses and limited area. Additionally, two different types of buses are considered, which means having at least two carports (one carport for each type) owing to their different geometries.

To solve this problem, this study proposes a multi-objective optimization model that determines the most cost-optimum design of the components of both the primary and secondary distribution systems of a large-scale electric bus depot. The optimization model uses the Mixed-Integer Quadratic Programming (MIQP) to reach the optimum solution regarding the predefined constraints. The selection of MIQP as a nonlinear method allows to consider nonlinear constraints. This enables the mathematical formulation of various parameters, that have nonlinear relations [18]. An electrical network consists of primary and secondary network. The primary grid is the network between the substation and distribution transformers, whereas the secondary grid is the network between the distribution transformers and loads. This optimization methodology considers the network as a group of modules. The selection of components is based on the objective of satisfying the technical aspects regarding the optimum costs. Modularization of the system facilitates standardization and scalability of the proposed solution at optimum costs [19].

Several sensitivity analyses are performed to obtain a general solution for this problem. The aim is to test the selection criteria for a circuit under various conditions. The unique contribution of this research is its ability to show the optimum design of the bus depot to bus operators by considering predefined routes, the types of available buses, and the area of the depot. The model presents in this study can determine the effect of varying the charging power on the requirements of the charging infrastructure. The main contributions of this paper are summarized as follows:

First, it proposes a multi-objective model for optimal planning the electric network of bus depots infrastructure.

Second, the proposed formulation ensures that the determined components are based on the optimal scheduling of buses. This guarantees an optimal peak load of the depot as well as minimum number of buses required to travel the routes.

Third, this framework enables the consideration of area limitations, which is an important constraint in large cities. Accordingly, the area is divided into two variables, which area the length and the width. By optimizing both variables, the optimum total area is concluded. For that reason, the geometry of the depot is considered as a rectangle.

Fourth, this framework considers the least number of components in an electrical power system of a bus depot. Consequently, this ensures planning the depot at minimum cost.

The problems addressed in this study are discussed in section II. Section III describes the methodology used in this study. The applied constraints are described in this section as well. In Section IV, the results of applying the model to a bus depot are presented, and the effects of implementing sensitivity studies on the calculated area, components of the electrical system, and configuration of the buses in the depot are observed. Finally, a conclusion and brief overview of future research are presented.

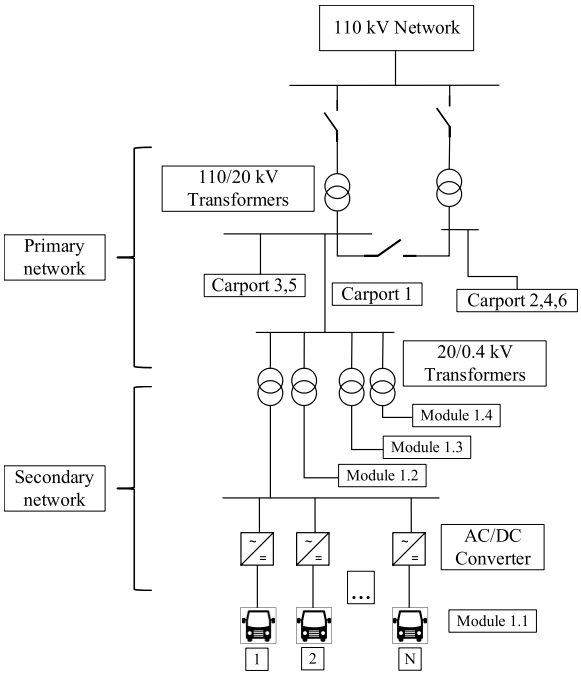

FIGURE 1. A conventional single line diagram of the electric bus depot [21].

II. PROBLEM DEFINITION

The main problem addressed in this study is the identification of the main variants that affect the electrification process of buses. Before using any optimization in the design, the status quo of the bus depot power system is presented as shown in FIGURE 1. The complexity of the problem for the proposed modules, is that they should result in the lowest possible system cost along with the system compatibility to the available area. The proposed solution divides the system into modules, that can be optimized according to its specific parameters. Consequently, each component in the system can be optimized, which satisfies the main objective of the algorithm to reduce the total cost.

The problem involves a group of continuous and binary variables. Continuous variables determine the number of system components, such as transformers, cables, and chargers. The binary variables are the decision variables that select the existence of each branch. This means, for example, whether it is essential to have a high voltage network. The variables are chosen to be content with predefined constraints to satisfy the objective function of the problem. The design problem is based on the successive construction of the system, in which the model generates a new search tree at each step. At each node, the model determines the optimal branch to consider its connection to the subsequent node [20]. The Gurobi solver is implemented to solve the entire tree by determining the optimal answer to the original MIQP problem.

III. METHODOLOGY

In comparison to other software tools for power system modelling in [22], [23], and [24], the model introduced in this study focuses on large-scale bus depots. Each class comprise a group of variables and methods. In the main class, the Graphical User Interface (GUI) is initialized to select the targeted depot. Based on this selection, the input data are read in the input class. With the help of sorting algorithms in the charger and route classes, the class schedule shows which bus shall travel each route. The load curve is calculated by summing up the charging power of buses charging at the same time. Afterward, all the data are fed into the optimization class to determine the number of components and draw the layout of the depot. In turn, the model includes calculating the peak load, which depends on the planned routes, and considers the area limitations. Subsequently, optimization constraints and objectives are implemented. All constraints are built depending on each component specific features. For instance, the selection of transformers is dependent on their power, voltage, price and foundation costs. Additionally, the number of transformers depends on the number of carports, as it is planned to supply each carport independently but in a ring system. A detailed overview of the model is presented in FIGURE 3. Mixed-Integer Programming (MIP) method is used to determine the optimal design of the depot in this study. In general, any MIP problem contains continuous variables and at least one integer. In some cases, the objective function does not include any quadratic term; hence, the problem is defined as Mixed-Integer Linear Programming (MILP). In other cases, only the constraints embrace quadratic terms. Therefore, the problem is represented as a Mixed Integer Quadratic Constrained Programming (MIQCP). In our case, both the constraints and the objective function are quadratic; thus, MIQP is implemented. The system is generally presented as a group of blocks, as illustrated in FIGURE 2. This figure summarizes the design process by connecting the structure of the higher-level information. The inputs of the system are listed on the left-hand side. These are the planned routes to be covered by the bus depot and the available areas for building the depot infrastructure. These inputs undergo the MIQP method by considering predefined constraints [25]. Eventually, the outputs of this progression are the essential components of the system, including the parameters and the minimum required number of each component. Finally, the depot is drawn according to the optimal selected solution, and the variables of the number and type of selected components are shown. In the following subsections, all the constraints and objectives of the model are explained.

A. CALCULATION OF PEAK LOAD

Routing is calculated according to the First-In, First-Out (FIFO) principle. This implies that the first bus entering the depot is charged to be ready to take the next route. The routes of one day are imported into the model with details of departure and arrival times, as shown in FIGURE 4. This

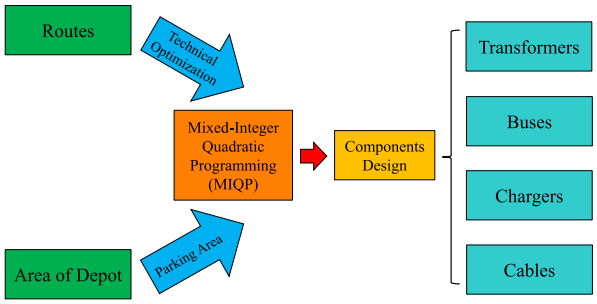

FIGURE 2. Block diagram of the modelling process starting from the available inputs to the depot design.

Gantt-chart shows that buses always travel different routes among the day, which in turn means different requirements for the charging infrastructure. The route ID, distance in kilometers, and type of bus needed are also included. Additionally, load of preheating the cabins of buses in winter is added. For this case, the worst-case scenario of having a temperature of -15 °C is implemented. Furthermore, no intelligent load management is applied. Accordingly, the charging schedule is concluded based on the availability of buses and their capability to travel the routes predefined [26]. Based on the route scheduling, the number of buses per type is calculated. According to constraints (1) and (2), the $H(t)$ represents the total height of power consumption of a complete day. sj is the start of the charging period and lj is the charging period, such that $sj + lj$ is the end of the charging process [27].

By implementing constraint (3), the peak load (P_{N}) is calculated by multiplying the maximum number of buses charging simultaneously ($H^{\max}$) by the charging power of one bus (P_{Ch}). Concurrently, the user is asked to enter the dimensions of the depot. These values are then fed in the form of constraints along with a database to the MIQP. This database contains various types of transformers and cables.

$$H(t) = \sum_{j:t\in[sj,sj+lj]} h_j \tag{1}$$

$$H^{\max} = \max_{t\in[0,\mathrm{T}]} H(t) \tag{2}$$

$$P_{\mathrm{N}} = P_{\mathrm{Ch}} \cdot H^{\max} \tag{3}$$

B. CONSTRAINTS ON THE AREA

To manage the available area, the optimization model calculates the possible number of rigid and articulated buses in both series and parallel arrangements. Simultaneously, free areas are integrated into the constraints. These free areas are significant for buses to be able to park in and out of their parking spaces. Area constraints are defined to include the number of free areas as a variable.

Constraints connect the variables of the number of carports to the variables of the number of free areas in a depot, so that each carport can be surrounded by free areas. Constraints (4) and (5) determine the geometric constraints on the width and length of the bus depot, which assumed to be a rectangular area as of the standard [28]. Generally, length constraints are

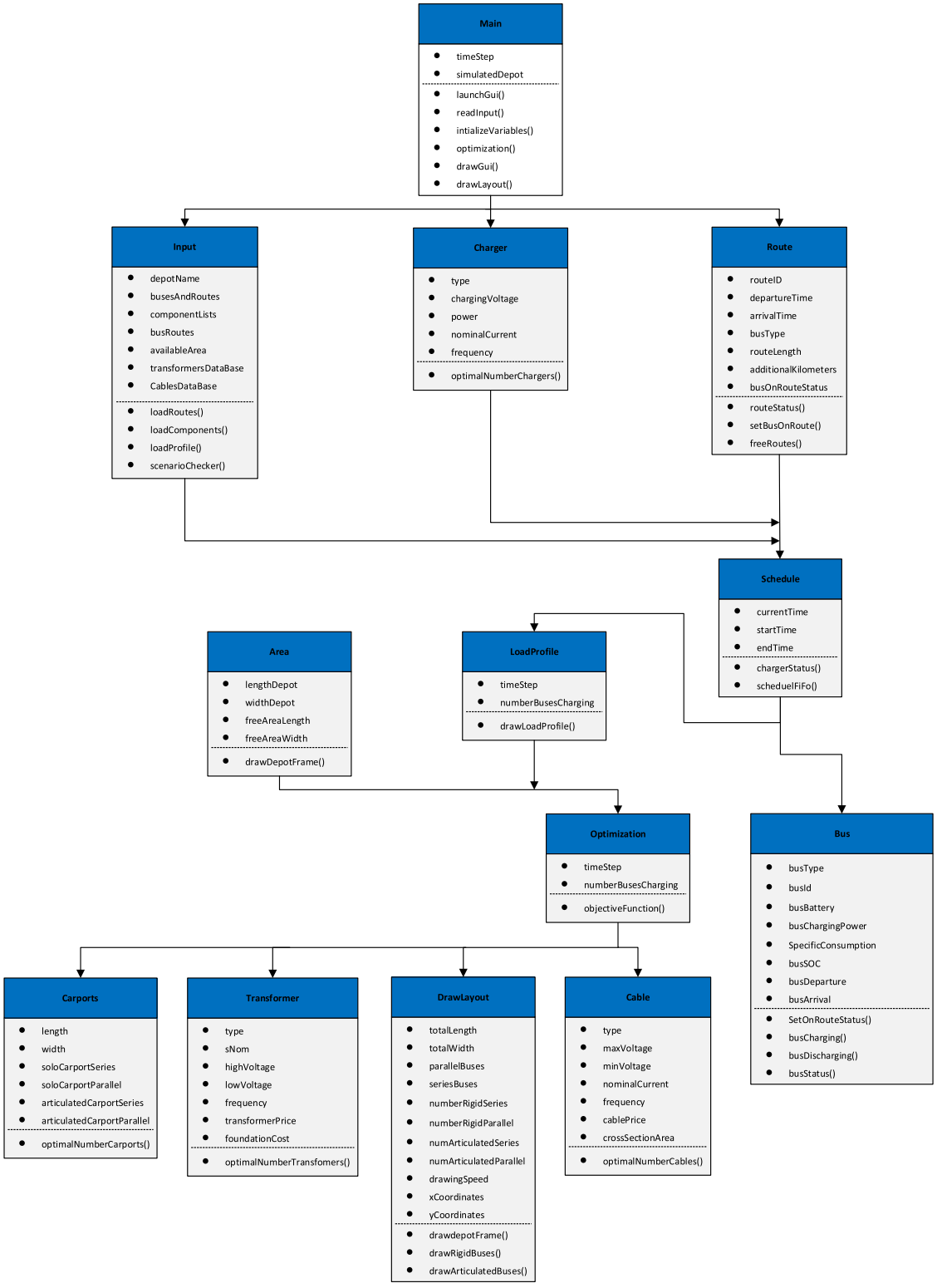

FIGURE 3. UML class diagram demonstrating the fundamental structure of the software framework which is programmed in the Python language used for building the optimization model.

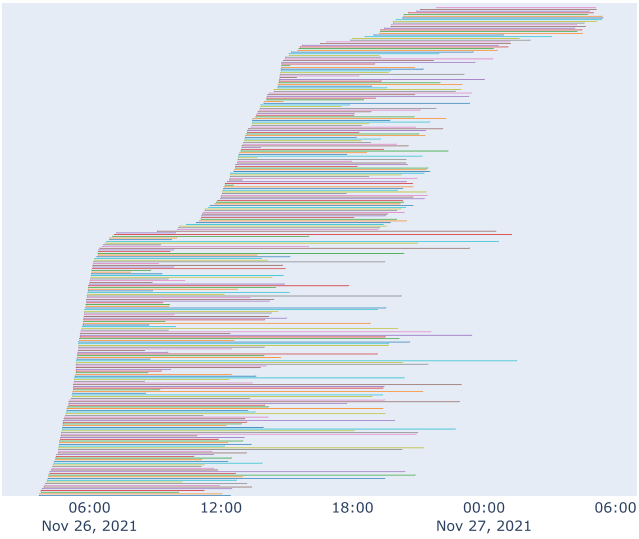

FIGURE 4. Representation of all the considered 287 routes of a bus depot for one day according to their departure and arrival times.

based on the fact, that the total length of the bus depot limits the number of buses that can be parked in series (behind each other). Concurrently, the total width of the depot limits the number of buses that can be parked in parallel (adjacent to each other). In constraint (6), the total area planned by the algorithm is limited to an area predefined by the user.

$$N_{\mathrm{TypP}} \cdot W_{\mathrm{Typ}} \cdot N_{\mathrm{TypCP}} + N_{\mathrm{TypCP}} \cdot W_{\mathrm{F}} \leq W_{\mathrm{D}} \tag{4}$$

$$N_{\mathrm{TypS}} \cdot L_{\mathrm{Typ}} \cdot N_{\mathrm{TypCS}} + N_{\mathrm{TypCS}} \cdot L_{\mathrm{F}} \leq L_{\mathrm{D}} \tag{5}$$

$$N_{\mathrm{Typ}} \cdot L_{\mathrm{Typ}} \cdot W_{\mathrm{Typ}} + N_{\mathrm{TypC}} \cdot L_{\mathrm{F}} \cdot W_{\mathrm{F}} \leq W_{\mathrm{D}} \cdot L_{\mathrm{D}} \tag{6}$$

The free area here ($L_{\mathrm{F}} \cdot W_{\mathrm{F}}$) is the area between carports, which is previously explained. In constraint (7), the number of free areas is defined along with the length of the possible series carports. Similarly, the number of free-area widths is defined in constraint (8). It is defined by two components, which are the number of lengths and the widths. Constraint (9) ensures that the number of selected lengths equals the number of the selected widths.

$$N_{\mathrm{FL}} \cdot L_{\mathrm{F}} + L_{\mathrm{Typ}} \cdot N_{\mathrm{TypS}} \leq L_{\mathrm{D}} \tag{7}$$

$$N_{\mathrm{FW}} \cdot W_{\mathrm{F}} + W_{\mathrm{Typ}} \cdot N_{\mathrm{TypP}} \leq W_{\mathrm{D}} \tag{8}$$

$$N_{\mathrm{FL}} = N_{\mathrm{FW}} \tag{9}$$

In constraints (10)-(12), the total lengths of the carports are formulated based on the predefined constants listed in TABLE 1, including variables that will be solved later. These constraints will not only be implemented in the geometry section but also later in calculating the lengths of the cables. Constraint (13) defines the total length required for the carport.

$$L_{\mathrm{TypC}} = N_{\mathrm{TypS}} \cdot L_{\mathrm{Typ}} \tag{10}$$

$$L_{\mathrm{TypTC}} = N_{\mathrm{TypC}} \cdot L_{\mathrm{TypC}} \tag{11}$$

$$L_{\mathrm{TypF}} = N_{\mathrm{TypCS}} \cdot L_{\mathrm{F}} \tag{12}$$

TABLE 1. List of the constants applied for defining the bus depot available area in terms of length and width, as well as the dimensions of used buses in the model.

Constant	Value
L_{D}	244 m
L_{F}	15 m
L_{Typ}	12 m (rigid buses)
	18 m (articulated buses)
P_{Ch}	150 kW
PF	0.85
V_{LV}	0.4 kV
W_{D}	136 m
W_{F}	1 m
W_{Typ}	3 m (rigid buses)
	3 m (articulated buses)

$$L_{\mathrm{TypT}} = L_{\mathrm{TypTC}} + L_{\mathrm{TypF}} \tag{13}$$

The same constraints are also applied to the widths through constraints (14)-(16). Constraint (17) defines the total width required for the carport.

$$W_{\mathrm{TypC}} = N_{\mathrm{TypP}} \cdot W_{\mathrm{Typ}} \tag{14}$$

$$W_{\mathrm{TypTC}} = N_{\mathrm{TypC}} \cdot W_{\mathrm{TypC}} \tag{15}$$

$$W_{\mathrm{TypF}} = N_{\mathrm{ABCP}} \cdot W_{\mathrm{F}} \tag{16}$$

$$W_{\mathrm{TypT}} = W_{\mathrm{TypTC}} + W_{\mathrm{TypF}} \tag{17}$$

By applying constraint (18), the number of carports is limited to be lower than the total number of buses of each bus type.

$$N_{\mathrm{TypC}} \leq N_{\mathrm{Typ}} \tag{18}$$

Additionally, constraints (19)-(20) ensure that at least one component for each variable is selected. Constraints (21)-(23) are the boundary constraints, that connect the number of series and parallel buses, either rigid or articulated buses, to the total number of buses.

$$N_{\mathrm{TypS}} \geq 1 \tag{19}$$

$$N_{\mathrm{TypP}} \geq 1 \tag{20}$$

$$N_{\mathrm{TypS}} \leq N_{\mathrm{Typ}} \tag{21}$$

$$N_{\mathrm{TypP}} \leq N_{\mathrm{Typ}} \tag{22}$$

$$N_{\mathrm{TypS}} \cdot N_{\mathrm{TypP}} = N_{\mathrm{Typper\ C}} \tag{23}$$

C. CONSTRAINTS ON THE NUMBER OF CARPORTS

Constraints (24)-(26) formulate the number of carports. By implementing constraint (24), the number of series and parallel carports is limited to the total possible number of carports for each bus type. Constraints (25)-(26) ensure, that the number of series and parallel carports remains within the predefined depot area.

$$N_{\mathrm{TypCP}} \cdot N_{\mathrm{TypCS}} = N_{\mathrm{TypC}} \tag{24}$$

$$N_{\mathrm{TypCS}} \cdot L_{\mathrm{Typ}} \leq L_{\mathrm{D}} \tag{25}$$

$$N_{\mathrm{TypCP}} \cdot W_{\mathrm{Typ}} \leq W_{\mathrm{D}} \tag{26}$$

D. CONSTRAINTS ON THE NUMBER OF CHARGERS

There are two methods to calculate the number of chargers. In the first method, the number of chargers is set equal to the total calculated number of buses. The second method is to limit the number of chargers to the number of buses charging at simultaneously. In this study, the first choice is selected, as shown in constraint (27) considering the utilization factor (UF). This is because swapping buses in the depot is accompanied by extra operational and manpower complexities.

$$N_{\mathrm{CH}} = (N_{\mathrm{Typ}}) \cdot \mathrm{UF} \tag{27}$$

E. CONSTRAINTS ON THE TRANSFORMERS

The model creates a chain of transformers, that satisfies the predefined constraints. As defined in constraint (28), if the maximum load exceeds 14 MW, voltage transformation starts at the high-voltage side (110 kV). Consequently, high-voltage transformers are selected proceeding to the medium-voltage level and then to the low-voltage side (0.4 kV) [29]. Otherwise, if the chain starts at a medium-voltage level (10 or 20 kV), the selection would start at this medium-voltage and then would proceed to the low-voltage level (0.4 kV).

$$V_{\mathrm{p,grid}} = \begin{cases} 110\ \mathrm{kV}; & \text{if } P_{\mathrm{N}} \geq 14\ \mathrm{MW} \\ 20\ \mathrm{kV}; & \text{if } P_{\mathrm{N}} < 14\ \mathrm{MW} \\ 10\ \mathrm{kV}; & \text{if } P_{\mathrm{N}} < 14\ \mathrm{MW} \end{cases} \tag{28}$$

The choice between 10 and 20 kV depends on the total cost of each system. Furthermore, the costs are defined as 15€/kVA, in addition to the assumed fixed foundation cost per transformer. Adding the foundation costs of the 150 k€ pro transformer to the calculation is beneficial for limiting the number of selected transformers to avoid irrational selections. The database of transformers is listed in TABLE 2, according to their powers, prices, and primary and secondary voltages. Constraint (29) defines the existence of at least one transformer at each voltage level. The term ($\theta_{i'}^{\mathrm{sTHV}}$) represents the existence of high-voltage transformers at the node (i'), which belongs to the set high voltage nodes (ψ). The binary decision variable ($\theta_{i'}^{\mathrm{sTyp}}$) represents the existence of transformers for the two types of buses in the set of nodes (Ω). It applies that all transformers are predefined in the set T_{P}.

$$\sum_{i' \in \psi} \theta_{i'}^{\mathrm{sTHV}} = \sum_{i' \in \Omega} \theta_{i'}^{\mathrm{sTyp}} = 1; \quad \mathrm{sTHV} \in T_{\mathrm{P}},\ \mathrm{sTyp} \in T_{\mathrm{P}} \tag{29}$$

Constraints (30)-(31) enable the absence of any voltage-level transformers if they do not exist. For example, if a bus depot requests only one type of bus, there is no need to plan transformers for the other.

$$\theta_{i'}^{\mathrm{sTHV}} = 0; \quad \text{if } N_{i'}^{\mathrm{sTHV}} = 0;\ i' \in \psi, \mathrm{sTHV} \in T_{\mathrm{P}} \tag{30}$$

$$\theta_{i'}^{\mathrm{sTyp}} = 0; \quad \text{if } N_{i'}^{\mathrm{sTyp}} = 0;\ i' \in \Omega, \mathrm{sTyp} \in T_{\mathrm{P}} \tag{31}$$

Constraints (32)-(33) are the boundary constraints, that connect the existence variable of each component to the chosen number of transformers. Constraint (34) bounds the total number of transformers in high-voltage or medium-voltage zones according to their existence. In constraint (35), the total number of transformers used for the rigid and articulated buses is also bounded according to their existence.

TABLE 2. Part of the transformers database used to select the most optimum transformer (T_{P}).

Type	Power (MVA)	$V_{i'}^{\mathrm{p}}$ (kV)	$V_{i'}^{\mathrm{s}}$ (kV)	Price (€)
0.1 MVA 10/0.4 kV	0.1	10	0.4	1500
⋮	⋮	⋮	⋮	⋮
0.1 MVA 20/0.4 kV	0.1	20	0.4	1500
⋮	⋮	⋮	⋮	⋮
0.16 MVA 10/0.4 kV	0.16	10	0.4	2400
⋮	⋮	⋮	⋮	⋮
0.16 MVA 20/0.4 kV	0.16	20	0.4	2400
⋮	⋮	⋮	⋮	⋮
0.2 MVA 10/0.4 kV	0.2	10	0.4	3000
⋮	⋮	⋮	⋮	⋮
63 MVA 110/20 kV	63	110	20	945,000
⋮	⋮	⋮	⋮	⋮

$$\theta_{i'}^{\mathrm{sTHV}} \cdot N_{i'}^{\mathrm{sTHV}} = N_{i'}^{\mathrm{sTHV}}; \quad i' \in \psi, \mathrm{sTHV} \in T_{\mathrm{P}} \tag{32}$$

$$\theta_{i'}^{\mathrm{sTyp}} \cdot N_{i'}^{\mathrm{sTyp}} = N_{i'}^{\mathrm{sTyp}}; \quad i' \in \Omega, \mathrm{sTyp} \in T_{\mathrm{P}} \tag{33}$$

$$\sum_{i' \in \psi} \theta_{i'}^{\mathrm{sTHV}} \cdot N_{i'}^{\mathrm{sTHV}} = \sum_{i' \in \psi} N_{i'}^{\mathrm{sTHV}}; \quad \mathrm{sTHV} \in T_{\mathrm{P}} \tag{34}$$

$$\sum_{i' \in \Omega} \theta_{i'}^{\mathrm{sTyp}} \cdot N_{i'}^{\mathrm{sTyp}} = \sum_{i' \in \Omega} N_{i'}^{\mathrm{sTyp}}; \quad \mathrm{sTyp} \in T_{\mathrm{P}} \tag{35}$$

The total power required for each carport depends on the number of buses charging at this carport. Subsequently, the number of transformers is planned based on the maximum power required to charge the buses at each carport and the number of carports for each bus type (rigid or articulated). In constraint (36), the selected number of transformers for buses carports (N_{TVTyp}) multiplied by the set of possible transformer powers defined previously in the data set ($P_{i'}^{\mathrm{T}}$) is set to equalize the number of buses per carport multiplied by the charging power per bus. This specifies the power required per carport.

$$N_{\mathrm{TVTyp}} \cdot P_{i'}^{\mathrm{T}} \geq N_{\mathrm{Typper\ C}} \cdot P_{\mathrm{Ch}}; \quad i' \in \Omega \tag{36}$$

Constraint (37) ensures that the total number of buses of each bus type is always equal to the total number of buses of that type per carport multiplied by the number of carports.

$$N_{\mathrm{Typper\ C}} \cdot N_{\mathrm{TypC}} = N_{\mathrm{Typ}} \tag{37}$$

In constraint (38), the number of transformers is set equal to or greater than the number of carports for each bus type. This would guarantee the planning of at least one transformer per carport to avoid connecting the carports at a low-voltage level.

$$\sum_{i' \in \Omega} \theta_{i'}^{\mathrm{sTyp}} \cdot N_{i'}^{\mathrm{sTyp}} \geq N_{\mathrm{TypC}}; \quad \mathrm{sTyp} \in T_{\mathrm{P}} \tag{38}$$

Constraint (39) ensures that the calculated capacity at the grid connection point is equal to or greater than the power required to supply all the buses.

$$\sum_{i' \in \Omega} \theta_{i'}^{\mathrm{sTyp}} \cdot N_{i'}^{\mathrm{sTyp}} \cdot P_{i'}^{\mathrm{T}} \geq P_{\mathrm{N}}; \quad \mathrm{sTyp} \in T_{\mathrm{P}} \tag{39}$$

The total power of the bus depot is calculated to define the voltage level of the transformers. If the maximum required power capacity exceeds 14 MW, the bus depot must be connected to the 110 kV-network. Otherwise, a connection to 20 kV or 10 kV would be sufficient, as previously mentioned in constraint (28).

Constraint (40) defines the power of the medium-voltage or high-voltage transformers. On the left-hand side, the existence variable of the medium-voltage ($\theta_{i'}^{\mathrm{sTHV}}$) is multiplied by the optimum number of transformers ($N_{i'}^{\mathrm{sTHV}}$) by the power of each transformer, which is predefined in the database of transformers ($P_{i'}^{\mathrm{T}}$). This term of the constraint is restricted to be more than or equal to the total power demand of the depot (P_{N}) on the right-hand side.

$$\sum_{i' \in \psi} \theta_{i'}^{\mathrm{sTHV}} \cdot N_{i'}^{\mathrm{sTHV}} \cdot P_{i'}^{\mathrm{T}} \geq P_{\mathrm{N}}; \quad \mathit{if}\ V_{\mathrm{p,grid}} = 110\,\mathrm{kV}, \quad \mathrm{sTHV} \in T_{\mathrm{P}} \tag{40}$$

Constraint (41) ensures that the primary voltage of the high-voltage transformer corresponds to the chosen voltage level at the grid connection point. This is done by multiplying the existence variable of the medium-voltage ($\theta_{i'}^{\mathrm{sTHV}}$) by the optimum number of transformers ($N_{i'}^{\mathrm{sTHV}}$) by the voltage of each transformer, which is predefined in the database of transformers ($V_{i'}^{\mathrm{p}}$) on the left-hand side.

On the right-hand side, the existence variable of the medium-voltage ($\theta_{i'}^{\mathrm{sTHV}}$) is multiplied by the optimum number of transformers ($N_{i'}^{\mathrm{sTHV}}$) by the optimum voltage at the grid point of connection ($V_{\mathrm{p,grid}}$). The target of this constraint is to limit the primary voltage of the transformer at the grid connection point to the chosen voltage of the medium-voltage network.

Constraint (42) calculates the secondary voltage of the high voltage transformers if they exist. This is achieved by bounding the algorithm to choose transformers whose voltages are larger than 0.4 kV but simultaneously lower than 110 kV, which are either 10 kV or 20 kV transformers. Constraint (43) ensures, that the secondary voltage of the transformer at the grid connection point is the primary voltage of the following distribution transformers for both bus types. As a result, each voltage level is connected to the following level forming a chain of transformers, that cope with the starting voltage at the point of connection with the grid to the low voltage side of the network. This is realized by equating the existence variable of the medium-voltage ($\theta_{i'}^{\mathrm{sTHV}}$) multiplied by the set of secondary voltages ($V_{i'}^{\mathrm{s}}$) to that of each bus type transformer ($\theta_{i'}^{\mathrm{sTyp}}$) multiplied by the set of primary voltages ($V_{i'}^{\mathrm{p}}$).

$$\left(\sum_{i' \in \psi} \theta_{i'}^{\mathrm{sTHV}} \cdot N_{i'}^{\mathrm{sTHV}}\right) \cdot \left(V_{i'}^{\mathrm{p}}\right) \geq \left(\sum_{i' \in \psi} \theta_{i'}^{\mathrm{sTHV}} \cdot N_{i'}^{\mathrm{sTHV}}\right) \cdot (V_{\mathrm{p,grid}}); \quad \mathit{if}\ V_{\mathrm{p,grid}} = 110\mathrm{kV}, \mathrm{sTHV} \in T_{\mathrm{P}}, \mathrm{p} \in T_{\mathrm{P}} \tag{41}$$

$$\left(\sum_{i' \in \psi} \theta_{i'}^{\mathrm{sTHV}} \cdot N_{i'}^{\mathrm{sTHV}}\right) \cdot \left(V_{i'}^{\mathrm{s}}\right) \geq \left(\sum_{i' \in \psi} \theta_{i'}^{\mathrm{sTHV}} \cdot N_{i'}^{\mathrm{sTHV}}\right) \cdot (V_{\mathrm{LV}}); \quad \mathit{if}\ V_{\mathrm{p,grid}} = 110\mathrm{kV}, \mathrm{sTHV} \in T_{\mathrm{P}}, \mathrm{s} \in T_{\mathrm{P}} \tag{42}$$

$$\sum_{i' \in \psi} \theta_{i'}^{\mathrm{sTHV}} \cdot V_{i'}^{\mathrm{s}} = \sum_{i' \in \Omega} \theta_{i'}^{\mathrm{sTyp}} \cdot V_{i'}^{\mathrm{p}}; \quad \mathit{if}\ V_{\mathrm{p,grid}} = 110\mathrm{kV}, \mathrm{sTHV} \in T_{\mathrm{P}}, \mathrm{sTyp} \in T_{\mathrm{P}}, \mathrm{p} \in T_{\mathrm{P}} \tag{43}$$

If the starting voltage is lower than 110 kV, distribution transformers would be selected directly. Constraint (44) drive the primary voltage of both bus types from the $V_{\mathrm{p,grid}}$ which, in this case, would be either 10 kV or 20 kV.

$$\sum_{i' \in \Omega} \theta_{i'}^{\mathrm{sTyp}} \cdot V_{i'}^{\mathrm{p}} = V_{\mathrm{p,grid}}; \mathit{if}\ V_{\mathrm{p,grid}} < 110\mathrm{kV}, \quad \mathrm{sTyp} \in T_{\mathrm{P}}, \mathrm{p} \in T_{\mathrm{P}} \tag{44}$$

To adjust the secondary voltage to 0.4 kV, constraint (45) is defined. This constraint takes out the 0.4 kV as a common factor in the equation (sum of all transformers voltages = sum of all transformers x 0.4 kV). Therefore, the calculated number of transformers on the low-voltage side is a multiple of 0.4 kV.

$$\left(\sum_{i' \in \Omega} \theta_{i'}^{\mathrm{sTyp}} \cdot N_{i'}^{\mathrm{sTyp}}\right) \cdot V_{i'}^{\mathrm{s}} = \left(\sum_{i' \in \Omega} \theta_{i'}^{\mathrm{sTyp}} \cdot N_{i'}^{\mathrm{sTyp}}\right) \cdot V_{\mathrm{LV}}; \quad \mathrm{sTyp} \in T_{\mathrm{P}}, \mathrm{s} \in T_{\mathrm{P}} \tag{45}$$

F. CONSTRAINTS ON THE CABLES

The next step is to select cables for the system. By knowing the voltages and the chosen number of transformers, the number of cables and their voltages is determined. The cable lengths are determined according to the geometry of selected carports. It is assumed that all components are installed on the roof of the carports. Therefore, the area of the transformers is neglected. Chargers are also planned to be installed on the rooftop, where cables pass through ducts to buses underneath. Therefore, the distance from the transformers to the chargers is calculated based on the dimensions of the buses and the distance between the ceiling and a bus itself. The model then builds a chain of cables according to the connection between the transformers at

TABLE 3. Part of the cables database used to select the most optimum chain of cables (T_C) [30].

Name	Cross-section area (mm^2)	Nominal current (kA)	Price (€/m)	Voltage (kV)
NYCWY 4x35/16 0.4	35	0.129	17	0.4
NYCWY 4x50/25 0.4	50	0.157	22	0.4
⋮	⋮	⋮	⋮	⋮
N2XSY 1x70/16 10kV	70	0.297	12	10
⋮	⋮	⋮	⋮	⋮
N2XSY 1x70/16 20kV	70	0.297	13	20
⋮	⋮	⋮	⋮	⋮
149-AL1/24-ST1A 110.0	149	0.47	105	110
⋮	⋮	⋮	⋮	⋮

the grid connection point up to the carports. Then the connection from the distribution transformers to the chargers follows. As listed in TABLE 3, the cables are listed in the database according to their cross-sectional area (mm^2), nominal current, price (€/m), and voltage (kV). Constraints (46)-(48) are boundary constraints, that ensure that at least one cable is planned for the high-voltage grid, as well as for each bus type and charger. Constraints (49)-(51) enable the absence of the cable types if they do not exist. For example, if a bus depot requests only one type of bus, it is not necessary to plan either the transformers or the connecting cables for the other type.

$$\sum_{(i,j)\in\psi} \theta_{ij}^{\mathrm{cHV}} = 1; \quad \mathrm{cHV} \in T_C \tag{46}$$

$$\sum_{(i,j)\in\Omega} \theta_{ij}^{\mathrm{cTyp}} = 1; \quad \mathrm{cTyp} \in T_C \tag{47}$$

$$\sum_{(i,j)\in\Pi} \theta_{ij}^{\mathrm{cCH}} = 1; \quad \mathrm{cCH} \in T_C \tag{48}$$

$$\theta_{ij}^{\mathrm{cHV}} = 0; \quad if\ N_{ij}^{\mathrm{cHV}} = 0;\ (i,j) \in \psi, \mathrm{cHV} \in T_C \tag{49}$$

$$\theta_{ij}^{cTyp} = 0; \quad if\ N_{ij}^{cTyp} = 0;\ (i,j) \in \Omega, cTyp \in T_C \tag{50}$$

$$\theta_{ij}^{\mathrm{cCH}} = 0; \quad if\ N_{ij}^{\mathrm{cCH}} = 0;\ (i,j) \in \Pi, \mathrm{cCH} \in T_C \tag{51}$$

Constraints (52)-(54) are boundary constraints, that connect the existence variable of each cable type to the chosen number of cables. An integer variable (N_{ij}^{cHV}) is introduced to determine the number of cables of each type in the high-voltage or medium-voltage zone. The same is done for each bus type and the chargers through (N_{ij}^{cTyp}), and (N_{ij}^{cCH}).

$$\theta_{ij}^{\mathrm{cHV}} \cdot N_{ij}^{\mathrm{cHV}} = N_{ij}^{\mathrm{cHV}}; \quad (i,j) \in \psi,\ \mathrm{cHV} \in T_C \tag{52}$$

$$\theta_{ij}^{\mathrm{cTyp}} \cdot N_{ij}^{\mathrm{cTyp}} = N_{ij}^{\mathrm{cTyp}}; \quad (i,j) \in \Omega,\ \mathrm{cTyp} \in T_C \tag{53}$$

$$\theta_{ij}^{\mathrm{cCH}} \cdot N_{ij}^{\mathrm{cCH}} = N_{ij}^{\mathrm{cCH}}; \quad (i,j) \in \Pi,\ \mathrm{cCH} \in T_C \tag{54}$$

Constraint (55) limits the total number of cables in high voltage, or medium-voltage zone based on the selected chain of transformers. Constraint (56) controls the total number of cables used for each type of bus. Constraint (57) implements the same limitation on the number of cables used for chargers.

$$\sum_{(i,j)\in\psi} \theta_{ij}^{\mathrm{cHV}} \cdot N_{ij}^{\mathrm{cHV}} = \sum_{(i,j)\in\psi} N_{ij}^{\mathrm{cHV}}; \quad \mathrm{cHV} \in T_C \tag{55}$$

$$\sum_{(i,j)\in\Omega} \theta_{ij}^{\mathrm{cTyp}} \cdot N_{ij}^{\mathrm{cTyp}} = \sum_{(i,j)\in\Omega} N_{ij}^{\mathrm{cTyp}}; \quad \mathrm{cTyp} \in T_C \tag{56}$$

$$\sum_{(i,j)\in\Pi} \theta_{ij}^{\mathrm{cCH}} \cdot N_{ij}^{\mathrm{cCH}} = \sum_{(i,j)\in\Pi} N_{ij}^{\mathrm{cCH}}; \quad \mathrm{cCH} \in T_C \tag{57}$$

The voltages of the cables are determined to be similar to the voltages of the selected transformers, starting from the high-voltage level or the medium-voltage level moving forward to the low-voltage level. Constraint (58) controls the cables of the high-voltage network. This is realized by multiplying the summation of the existence binary variable of the types of cables $\theta_{ij}^{\mathrm{cHV}}$ by the integer variable N_{ij}^{cHV}, which determines the selected number of each cable type, multiplied by the set of cable databases V_{ij}^{c}, on the left-hand side. On the right-hand side, the same parameters of $\theta_{ij}^{\mathrm{cHV}}$ and N_{ij}^{cHV} are multiplied by the term (V_{LV}), which represent the voltages above the low voltage level (0.4 kV). Additionally, constraint (59) ensures that all the voltage levels below the ($V_{\mathrm{p,grid}}$) are covered in case ($V_{\mathrm{p,grid}} = 110$ kV) as a complementary step for the previous constraint. Constraint (60) controls the selection of cables in the low-voltage network, that are used to connect the distribution transformers on the roof of each carport with the chargers. This is performed by multiplying the integer variable for the carport cables ($\theta_{ij}^{\mathrm{cTyp}}$) by the number of carports of each bus type (N_{ij}^{cTyp}) selected voltage for the secondary side ($V_{i'}^{s}$), from which the simulation selects the cables on the left-hand side. On the right-hand side, the same variants are introduced but multiplied by the V_{LV} which is predefined to be the low-voltage level (0.4 kV). Constraints (61) and (62) calculate the power of the selected transformers at the grid point of connection. Furthermore, the power of the transformers at the grid connection point is set to be greater than the total consumption of the depot and, consequently, greater than the consumption of both bus types using constraints (63) and (64). In constraints (65)-(67), the power required per transformer for each bus type is defined as a preparatory step for calculating the current flowing in the cables. Constraint (68) saves the secondary voltage of the high-or medium-voltage transformer to the variable voltage (V_{SHV}). Afterward, constraint (69) ensures that the chosen cable voltage matches the (V_{SHV}).

$$\sum_{(i,j)\in\psi} \theta_{ij}^{\mathrm{cHV}} \cdot N_{ij}^{\mathrm{cHV}} \cdot V_{ij}^{c} \geq \left(\sum_{(i,j)\in\psi} \theta_{ij}^{\mathrm{cHV}} \cdot N_{ij}^{\mathrm{cHV}} \right)$$

$$\cdot\ (V_{\mathrm{LV}})\,; \quad if\ V_{\mathrm{p,grid}} = 110\,\mathrm{kV}, j \in \psi,\ \mathrm{cHV} \in T_{\mathrm{C}},\ \mathrm{c} \in T_{\mathrm{C}} \tag{58}$$

$$\sum_{(i,j)\in\psi} \theta_{ij}^{\mathrm{cHV}} \cdot N_{ij}^{\mathrm{cHV}} \cdot V_{ij}^{\mathrm{c}} \leq \left(\sum_{(i,j)\in\psi} \theta_{ij}^{\mathrm{cHV}} \cdot N_{ij}^{\mathrm{cHV}}\right) \cdot \left(V_{\mathrm{p,grid}}\right); \quad if\ V_{\mathrm{p,grid}} = 110\,\mathrm{kV},\ \mathrm{cHV} \in T_{\mathrm{C}},\ \mathrm{c} \in T_{\mathrm{C}} \tag{59}$$

$$\left(\sum_{(i,j)\in\Omega} \theta_{ij}^{\mathrm{cTyp}} \cdot N_{ij}^{\mathrm{cTyp}}\right) \cdot V_{i'}^{\mathrm{s}} = \left(\sum_{(i,j)\in\Omega} \theta_{ij}^{\mathrm{cTyp}} \cdot N_{ij}^{\mathrm{cTyp}}\right) \cdot V_{\mathrm{LV}}; \quad i' \in \Omega,\ \mathrm{cTyp} \in T_{\mathrm{C}},\ \mathrm{s} \in T_{\mathrm{P}} \tag{60}$$

$$P_{\mathrm{THV}} = \sum_{(i,j)\in\psi} \theta_{ij}^{\mathrm{cHV}} \cdot P_{i'}^{\mathrm{T}}; \quad \mathrm{cHV} \in T_{\mathrm{C}},\ i' \in \psi \tag{61}$$

$$\sum_{i'\in\psi} N_{i'}^{\mathrm{sTHV}} \cdot P_{\mathrm{THV}} = \sum_{i'\in\psi} N_{i'}^{\mathrm{sTHV}} \cdot P_{i'}^{\mathrm{T}}; \quad \mathrm{sTHV} \in T_{\mathrm{P}} \tag{62}$$

$$P_{\mathrm{THV}} \geq P_{\mathrm{N}} \tag{63}$$

$$P_{\mathrm{THV}} \geq \left(\sum_{i'\in\Omega} \theta_{i'}^{\mathrm{sTyp}} \cdot N_{i'}^{\mathrm{sTyp}} \cdot P_{i'}^{\mathrm{T}}\right); \quad \mathrm{sTyp} \in T_{\mathrm{P}} \tag{64}$$

$$\sum_{i'\in\Omega} N_{i'}^{\mathrm{sTyp}} \cdot P_{\mathrm{Typ}} = \sum_{i'\in\Omega} N_{i'}^{\mathrm{sTyp}} \cdot P_{i'}^{\mathrm{T}}; \quad \mathrm{sTyp} \in T_{\mathrm{P}} \tag{65}$$

$$\sum_{i'\in\Omega} \theta_{i'}^{\mathrm{sTyp}} \cdot P_{\mathrm{Typ}} \cdot P_{i'}^{\mathrm{T}} \geq P_{\mathrm{TypC}}; \quad \mathrm{sTyp} \in T_{\mathrm{P}} \tag{66}$$

$$\sum_{i'\in\Omega} N_{i'}^{\mathrm{sTyp}} \cdot P_{\mathrm{Typ}} \geq P_{\mathrm{TypC}}; \quad \mathrm{sTyp} \in T_{\mathrm{P}} \tag{67}$$

$$V_{\mathrm{SHV}} = \sum_{i'\in\psi} \theta_{i'}^{\mathrm{sTHV}} \cdot V_{i'}^{\mathrm{s}}; \quad \mathrm{sTHV} \in T_{\mathrm{P}},\quad \mathrm{s} \in T_{\mathrm{P}} \tag{68}$$

$$\sum_{(i,j)\in\psi} \theta_{ij}^{\mathrm{cHV}} \cdot V_{ij}^{\mathrm{c}} = V_{\mathrm{SHV}}; \quad \mathrm{cHV} \in T_{\mathrm{C}},\ \mathrm{c} \in T_{\mathrm{C}} \tag{69}$$

Constraints (70)-(72) calculates the current flowing in the cables at each network stage. This is performed by multiplying the existence variable of each cable type by the set of ampacities of the cables, which is predefined in the cables-database on the right-hand side. This is set to be equal to the current flowing in the cable on the left-hand side.

$$\sum_{(i,j)\in\psi} \theta_{ij}^{\mathrm{cHV}} \cdot I_{ij}^{\mathrm{c}} \geq \frac{P_{\mathrm{THV}}}{\sqrt{3}\cdot V_{\mathrm{SHV}} \cdot \mathrm{PF}}; \quad \mathrm{cHV} \in T_{\mathrm{C}},\ \mathrm{c} \in T_{\mathrm{C}} \tag{70}$$

$$\sum_{(i,j)\in\Omega} \theta_{ij}^{\mathrm{cTyp}} \cdot I_{ij}^{\mathrm{c}} \geq \frac{P_{\mathrm{Typ}}}{\sqrt{3}\cdot V_{\mathrm{LV}} \cdot \mathrm{PF}}; \quad \mathrm{cTyp} \in T_{\mathrm{C}},\ \mathrm{c} \in T_{\mathrm{C}} \tag{71}$$

$$\sum_{(i,j)\in\Pi} \theta_{ij}^{\mathrm{cCH}} \cdot I_{ij}^{\mathrm{c}} \geq \frac{P_{\mathrm{Ch}}}{\sqrt{3}\cdot V_{\mathrm{LV}} \cdot \mathrm{PF}}; \quad \mathrm{cCH} \in T_{\mathrm{C}},\ \mathrm{c} \in T_{\mathrm{C}} \tag{72}$$

Constraints (73)-(75) control the cable lengths for both bus types by considering the geometry calculated by the model. In constraint (73), the number of carports (N_{TypC}) is multiplied by the number of buses per carport by the sum of the length and width of the rigid bus. The entire term (L_{TypCC}), which represents the length of cables required for rigid buses, is afterward multiplied by the existence binary variable ($\theta_{ij}^{\mathrm{cTyp}}$), which determines the selected types of cables. The same procedure is followed for the articulated buses. A length of only 1 m is added to the lengths of the buses to consider the small distance between the park slots (already included in the lengths of buses: L_{Typ}).

$$L_{\mathrm{TypCC}} = N_{\mathrm{TypC}} \cdot N_{\mathrm{TypperC}} \cdot (L_{\mathrm{Typ}} + W_{\mathrm{Typ}}) \tag{73}$$

$$N_{ij}^{\mathrm{cTyp}} \geq \theta_{ij}^{\mathrm{cTyp}} \cdot \left(L_{\mathrm{TypCC}}\right); \quad (i,j) \in \Omega,\ \mathrm{cTyp} \in T_{\mathrm{C}} \tag{74}$$

$$N_{ij}^{\mathrm{cCH}} \geq \theta_{ij}^{\mathrm{cCH}} \cdot (N_{\mathrm{CH}})\,; \quad (i,j) \in \Pi,\ \mathrm{cCH} \in T_{\mathrm{C}} \tag{75}$$

In the following step, the high-or medium-voltage cables are calculated using constraints (76)-(80). As they should be routed from the grid connection point to each carport, the total lengths are considered. Constraint (80) calculates the total needed length of cables as the number of needed 1 m cables. This is achieved by multiplying the existence variable ($\theta_{ij}^{\mathrm{cHV}}$) by the path of the cable, which is the length and width of the bus depot.

$$L_{\mathrm{TSC}} = N_{\mathrm{TypCS}} \cdot N_{\mathrm{TypS}} \cdot L_{\mathrm{Typ}} + N_{\mathrm{TypCS}} \cdot L_{\mathrm{F}} \tag{76}$$

$$L_{\mathrm{TCC}} = L_{\mathrm{TSC}} \cdot (N_{\mathrm{TypC}} + N_{\mathrm{TypC}})/2 \tag{77}$$

$$W_{\mathrm{TPC}} = N_{\mathrm{TypCP}} \cdot N_{\mathrm{TypP}} \cdot W_{\mathrm{Typ}} + N_{\mathrm{TypCP}} \cdot W_{\mathrm{F}} \tag{78}$$

$$W_{\mathrm{TCC}} = W_{\mathrm{TPC}} \cdot (N_{\mathrm{TypC}})/2 \tag{79}$$

$$N_{ij}^{\mathrm{cHV}} \geq \theta_{ij}^{\mathrm{cHV}} \cdot (L_{\mathrm{TCC}} + W_{\mathrm{TCC}})\,; \quad (i,j) \in K \tag{80}$$

G. OBJECTIVE FUNCTION

The objective of this optimization model, as mentioned previously, is to optimize the number of components at each voltage level. Moreover, to choose the minimum cost at each step, which leads to the most optimum expenses for the entire system. This is directly connected to the optimum planning of the available area. In constraint (81), the minimum cost for high-voltage transformers (C_{THV}) is calculated. This is achieved by multiplying the existence binary variable ($\theta_{ij}^{\mathrm{sTHV}}$) of each transformer type by the calculated number of selected transformers ($N_{i'}^{\mathrm{sTHV}}$) multiplied by the cost of each.

$$C_{\mathrm{THV}} = \sum_{i'\in\psi} \theta_{i'}^{\mathrm{sTHV}} \cdot N_{i'}^{\mathrm{sTHV}} \cdot CP_{i'}^{\mathrm{T}}; \quad \mathrm{sTHV} \in T_{\mathrm{P}} \tag{81}$$

Similarly, the costs of the transformers for bus types are calculated by multiplying the existence variables of each

($\theta_{i'}^{\mathrm{sTyp}}$) by the chosen number of each type ($N_{i'}^{\mathrm{sTyp}}$) by their costs from the set of transformers ($CP_{i'}^{\mathrm{T}}$), as defined in constraint (82).

$$C_{\mathrm{Typ}} = \sum_{i' \in \Omega} \theta_{i'}^{\mathrm{sTyp}} \cdot N_{i'}^{\mathrm{sTyp}} \cdot CP_{i'}^{\mathrm{T}}; \quad \mathrm{sTyp} \in T_{\mathrm{P}} \tag{82}$$

Furthermore, the cost of the cables is calculated based on the optimum cost. This is realized for the medium-voltage network by multiplying the existence binary variable ($\theta_{ij}^{\mathrm{cHV}}$) by the number of planned cables (N_{ij}^{cHV}) times the cost of each cable type (CP_{ij}^{c}), as shown in constraint (83). Correspondingly, constraint (84) ensures the optimum cost of the cables used for bus types.

$$C_{\mathrm{cHV}} = \sum_{(i,j) \in \psi} \theta_{ij}^{\mathrm{cHV}} \cdot N_{ij}^{\mathrm{cHV}} \cdot CP_{ij}^{\mathrm{c}}; \quad \mathrm{cHV} \in T_{\mathrm{C}},\ \mathrm{c} \in T_{\mathrm{C}} \tag{83}$$

$$C_{\mathrm{cTyp}} = \sum_{(i,j) \in \Omega} \theta_{ij}^{\mathrm{cTyp}} \cdot N_{ij}^{\mathrm{cTyp}} \cdot CP_{ij}^{\mathrm{c}}; \quad \mathrm{cTyp} \in T_{\mathrm{C}},\ \mathrm{c} \in T_{\mathrm{C}} \tag{84}$$

To sum up all system costs, transformer costs are added to form the term ($C_{\mathrm{Transformer}}$), as shown in Equation (85). In addition, all cable costs are added to form the term (C_{Cable}), as shown in equation (86).

$$C_{\mathrm{Transformer}} = C_{\mathrm{THV}} + C_{\mathrm{Typ}} \tag{85}$$

$$C_{\mathrm{Cable}} = C_{\mathrm{cHV}} + C_{\mathrm{cTyp}} \tag{86}$$

Finally, the area is considered as the objective function. This is realized by setting the objective to minimize the occupied depot length and width (min ($L_{\mathrm{TSC}} + W_{\mathrm{TPC}} + N_{\mathrm{TypS}} + N_{\mathrm{TypP}}$)) along with minimizing the costs of the cables and transformers, as shown in the objective function (87).

$$\min\left(C_{\mathrm{Cable}} + C_{\mathrm{Transformer}} + L_{\mathrm{TSC}} + W_{\mathrm{TPC}} + N_{\mathrm{TypS}} + N_{\mathrm{TypP}}\right) \tag{87}$$

IV. RESULTS

To solve the defined constraints of the MIQP problem, the code is written in Python 3.8. The Gurobi 9.1.2 optimization solver is used, running on a workstation with an Intel Xeon processor with a clock speed of 3.70 GHz, 4 cores and 16 GB RAM. As shown in FIGURE 5, the calculated total load is 11.25 MW, the peak load of the rigid buses is 4.58 MW and that of the articulated buses is 6.67 MW. Nevertheless, these results are bounded to the current predefined routes, which can only solve the predefined problem temporarily with no permissibility for extensions. For this reason, an extra 25% of the total load is added to consider a design safety factor and permits an opportunity for possible increase in the total load. This leads to the total power of 14.06 MW, which exceeds 14 MW, consisting of 5.72 MW for rigid buses and 8.34 MW for articulated buses. This guides the model to choose a primary voltage of 110 kV. An additional variant for the sensitivity case study is firefighting precautions in bus depots. As the area of roofs on which electrical equipment is installed increases, firefighting precautions become more complex [31]. Therefore, the area is limited to a study case to the maximum of 48 rigid buses or 40 articulated buses per carport to observe their effects on other components.

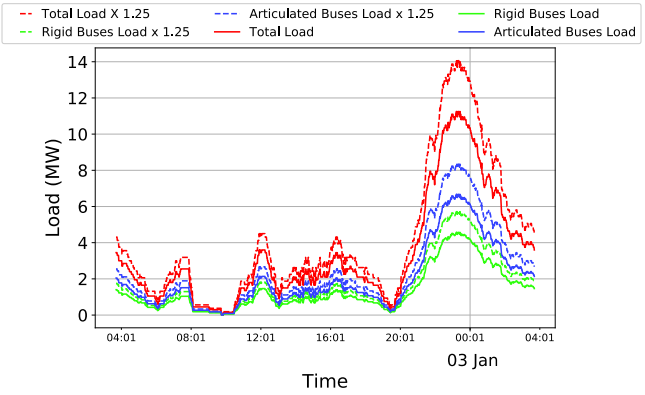

FIGURE 5. The load profile of the modelled bus depot where the charging load of rigid buses, articulated buses and the total load are calculated over a period of 24 h after adding a 25% design safety factor.

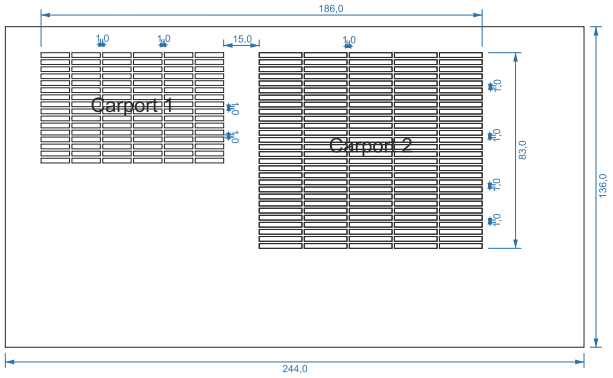

FIGURE 6. Distribution of buses among the available area without implementing the firefighting precautions.

A. IN CASE OF OPTIMIZING THE COSTS AND THE AREA

In the first optimization case, the objectives are defined to minimize the planned area as much as possible along with minimizing the system costs. As shown in TABLE 4, the calculated number of buses that can cover the predefined routes is 236, which implies 236 chargers. The results show 96 rigid and 140 articulated buses, distributed among two carports. The model plans the depot area to consist of one carport for rigid buses and one carport for the articulated buses. As shown in FIGURE 6, there are six rigid buses in series and 16 in parallel. Among the articulated buses, there are five buses planed in series and 28 buses in parallel. As shown in FIGURE 7, the single-line diagram of the bus depot is adapted to the results. The total effective length calculated is 186 m, which represents 76.23% of the total length, and a width of 83 m, representing 61.03% of the total width.

TABLE 4. The results of the considered variables in the prior mentioned constraints indicating the optimum components.

Variable	Value	Unit
N_{Typ}	96	rigid buses
	140	articulated buses
N_{TypS}	6	series rigid buses
	5	series articulated buses
N_{TypP}	16	parallel rigid buses
	28	parallel articulated buses
$N_{\mathrm{Typ\ per\ C}}$	96	rigid buses per carport
	140	articulated buses per carport
N_{TypCS}	1	series rigid buses carport
	1	series articulated buses carport
N_{TypCP}	1	parallel rigid buses carport
	1	parallel articulated buses carport
N_{ij}^{sTHV}	1 x 25 MVA 110/20 kV	transformers
P_{THV}	25	MVA
P_{Typ}	2	MVA for rigid buses transformer
	2	MVA for articulated buses transformer
N_{TVTyp}	3 x 2 MVA 20/0.4 kV	rigid buses transformers
	5 x 2 MVA 20/0.4 kV	articulated buses transformers
N_{ij}^{cHV}	339 m x N2XSH 1x500/35 20 kV	cables
N_{ij}^{cTyp}	1536 m x NSGAFÖU 4 x (4 x 1 x 300 mm²) 0.4 kV	rigid buses cables
	3080 m x NSGAFÖU 4 x (4 x 1 x 300 mm²) 0.4 kV	articulated buses cables
N_{ij}^{cCH}	4720 m x NYCWY 4 x 120/70 0.4 kV	cables
V_{SHV}	20	kV
C_{Total}	2,909,210	€
L_{TSC}	186	m
W_{TPC}	83	m

Subsequently, the electrical components of the system were determined. Based on the chosen components, the total cost is calculated, which helps to determine the optimum solution.

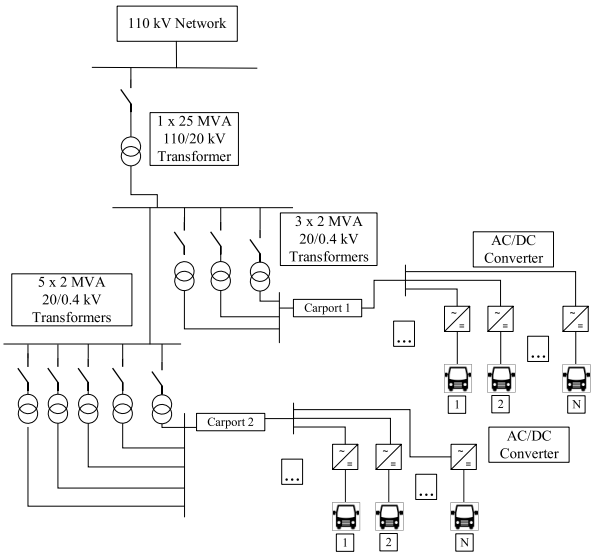

FIGURE 7. Single line diagram of the electrical power system of a bus depot, considering the objective of minimizing the available area along with minimizing the total system cost.

For medium voltage, a 25 MVA transformer is planned to supply the depot at 20 kV, which is then transformed using distribution transformers to 0.4 kV. For the carports of rigid buses, three transformers of type 2 MVA are planned, as well as five transformers of the same type for articulated buses.

B. IN CASE OF OPTIMIZING THE COSTS AND THE AREA CONSIDERING THE FIREFIGHTING PRECAUTIONS

In the second case, the objectives remain the same as the first case, that is, to minimize the area used and to minimize the total cost of the depot. Additionally, firefighting precautions are included. These precautions include planning less buses per carport to facilitate the role of firefighters in case of conflagrations. The area of the carports is controlled by limiting the number of buses per carport. Constraint (88) implements a real case limitation (N_{Limit}) for rigid buses, not to exceed 48 and for articulated buses, not to exceed 40.

$$N_{\mathrm{TypperC}} \leq N_{\mathrm{Limit}} \tag{88}$$

Correspondingly, the number of chargers is the same. However, additional constraints lead to an increase in the number of carports. For rigid buses, two carports are planned in parallel, whereas four carports are planned for articulated buses also in parallel. This leads to an increase in the occupied area of the depot, as shown in FIGURE 8. The total effective length calculated is 212 m, representing 86.88% of the total length, and a width of 86 m, representing 63.23% of the total width.

Similarly, the electrical components of the system are determined. For medium voltage, a 25 MVA transformer is

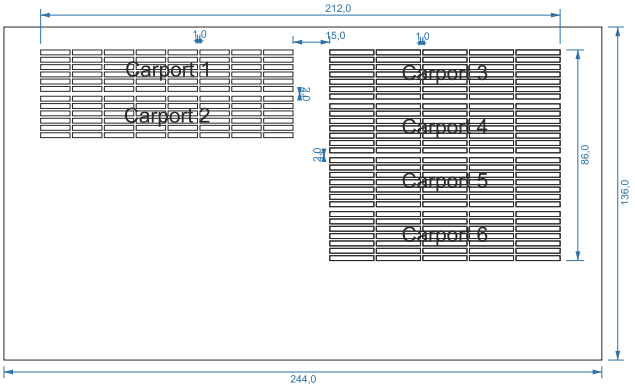

FIGURE 8. Distribution of buses among the available area with implementing the firefighting precautions investigating the number of carports.

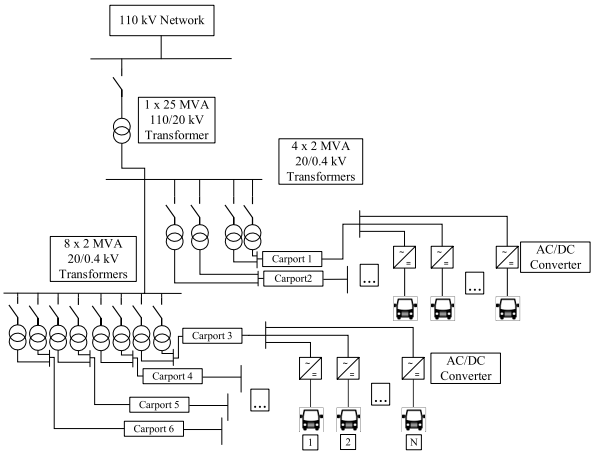

FIGURE 9. The single line diagram of the electrical power system of a bus depot, considering the area limiting constraints.

planned to supply the depot at 20 kV, which is then transformed using distribution transformers to 0.4 kV.

For the carports of the rigid buses, four transformers of type 2 MVA (two transformers per carport) are planned, along with eight. While, for the articulated buses transformers of type 2 MVA (two transformers per carport) are planned. In addition, the types and lengths of the cables are determined, and the total cost of the system is calculated. As shown in TABLE 5, the number of buses did not change because they are dependent on the predefined routes by the bus operator. As shown in FIGURE 9, the single-line diagram of the bus depot is adapted to the results.

C. IN CASE OF EXTENDING THE FIREFIGHTING PRECAUTIONS

In the third case, the objectives remain applied on the system as of the second case, except for the firefighting precautions. The security level is enhanced by reducing the number of buses parking at the same carport, as represented in constraint (89). Here the N_{Limit} is set not exceed 36 for rigid buses, not to exceed 30 buses for articulated buses. As shown in TABLE 6, the design of the charging infrastructure is affected on both sides of the electrical and geometrical aspects. On the geometrical aspect, all buses are distributed differently. This can be observed as of the increase in the number of carports

TABLE 5. The results of the considered variables, including the implementation of the area limiting constraints.

Variable	Value	Unit
N_{Typ}	96	rigid buses
	140	articulated buses
N_{TypS}	8	series rigid buses
	5	series articulated buses
N_{TypP}	6	parallel rigid buses
	7	parallel articulated buses
$N_{\text{Typ per C}}$	48	rigid buses per carport
	35	articulated buses per carport
N_{TypCS}	1	series rigid buses carport
	1	series articulated buses carport
N_{TypCP}	2	parallel rigid buses carport
	4	parallel articulated buses carport
$N_{ij}^{s\text{THV}}$	1 x 25 MVA 110/20 kV	transformer
P_{THV}	25	MVA
P_{Typ}	2	MVA for rigid buses transformer
	2	MVA for articulated buses transformer
N_{TVTyp}	4 x 2 MVA 20/0.4 kV	transformers
	8 x 2 MVA 20/0.4 kV	transformers
N_{ij}^{cHV}	1080 m x N2XSH 1 x 500/35 20kV	cables
N_{ij}^{cTyp}	1536 m x NSGAFÖU 4 x (4 x 1 x 300 mm²) 0.4 kV	cables
	3080 m x NSGAFÖU 4 x (4 x 1 x 300 mm²) 0.4 kV	cables
N_{ij}^{cCH}	4720 m x NYCWY 4 x 120/70 0.4 kV	cables
V_{SHV}	20	kV
C_{Total}	2,971,743	€
L_{TSC}	212	m
W_{TPC}	86	m

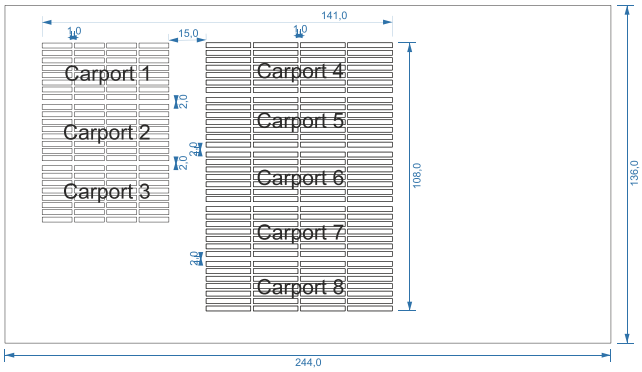

FIGURE 10. Distribution of buses among the available area with extending the firefighting, precautions investigating the number of carports.

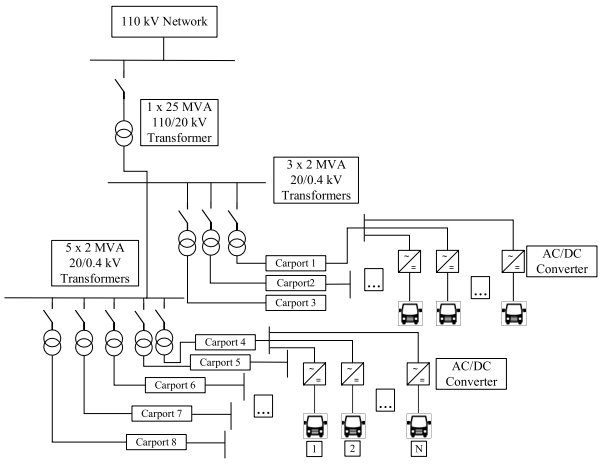

FIGURE 11. The single line diagram of the electrical power system of a bus depot, considering the extended area limiting constraints.

for both bus types, as shown in FIGURE 10. On the electrical design aspect, the number of transformers needed decreased for both bus types in comparison with last case, but the length of needed cables increased remarkably to adapt with the geometrical changes as shown in FIGURE 11.

$$N_{\text{TypperC}} \leq N_{\text{Limit}} \tag{89}$$

This leads to an increase in the total costs of the system Consequently, this motivated the study of possibilities to reduce the number of buses blocking each other, as discussed in the following case. Nevertheless, the total effective length calculated is 141 m, representing 57.78% of the total length, and a width of 108 m, representing 79.41% of the total width.

D. IN CASE OF MINIMIZING THE BLOCKING IN PARKING PLACE

In the fourth case, all constraints and objectives are still applied on the system, but the number of series rigid buses is restricted additionally. This helps in reducing the blocking of buses to each other, that accordingly simplifies the disposition problems of buses as represented in constraint (90). As shown

TABLE 6. The results of the considered variables with implementing higher level of firefighting.

Variable	Value	Unit
N_{Typ}	96	rigid buses
	140	articulated buses
N_{TypS}	4	series rigid buses
	4	series articulated buses
N_{TypP}	8	parallel rigid buses
	7	parallel articulated buses
$N_{\text{Typ per C}}$	32	rigid buses per carport
	28	articulated buses per carport
N_{TypCS}	1	series rigid buses carport
	1	series articulated buses carport
N_{TypCP}	3	parallel rigid buses carport
	5	parallel articulated buses carport
$N_{i'}^{s\text{THV}}$	1 x 25 MVA 110/20 kV	transformers
P_{THV}	25	MVA
P_{Typ}	2	MVA for rigid buses transformer
	2	MVA for articulated buses transformer
N_{TVTyp}	3 x 2 MVA 20/0.4 kV	rigid buses transformers
	5 x 2 MVA 20/0.4 kV	articulated buses transformers
N_{ij}^{cHV}	1404 m x N2XSH 1 x 500/35 20kV	cables
N_{ij}^{cTyp}	1536 m x NSGAFÖU 4 x (4 x 1 x 300 mm²) 0.4 kV	cables
	3080 m x NSGAFÖU 4 x (4 x 1 x 300 mm²) 0.4 kV	cables
N_{ij}^{cCH}	4720 m x NYCWY 4 x 120/70 0.4 kV	cables
V_{SHV}	20	kV
C_{Total}	2,998,694	€
L_{TSC}	141	m
W_{TPC}	108	m

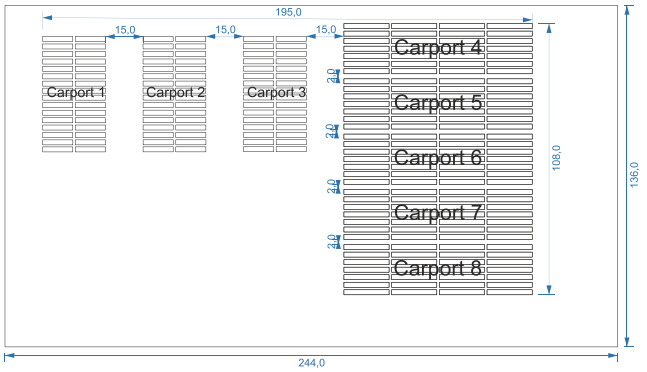

FIGURE 12. The single line diagram of the electrical power system of a bus depot, considering the case of minimizing blocking in parking place.

FIGURE 13. Comparison between the results of the four proposed sensitivity case studies (A-D) according to their cost, number of transformers, length of cables, number of carports, and occupied area.

in FIGURE 12, the design of the infrastructure is affected mainly on the geometrical aspect. This influences the electrical design and the total system cost as well, as shown in TABLE 7.

$$N_{\mathrm{TypS}} \leq 3 \tag{90}$$

Due to the spreading of carports over the area in comparison with previous cases, longer cables are needed between the point of connection with the grid and the carports. However, the number of transformers and their connection remain the same as the presented design in the last case, as previously shown in FIGURE 11.

As shown in FIGURE 13, results of sensitivity case studies (A-D) are plotted according to their planned cost, number of transformers, length of cables, number of carports and occupied area. These results can help bus operators to estimate their optimization priorities, knowing their effect on other design parameters.

TABLE 7. The results of the considered variables with minimizing blocking in parking place.

Variable	Value	Unit
N_{Typ}	96	rigid buses
	140	articulated buses
N_{TypS}	2	series rigid buses
	4	series articulated buses
N_{TypP}	16	parallel rigid buses
	7	parallel articulated buses
$N_{\mathrm{Typ\ per\ C}}$	32	rigid buses per carport
	28	articulated buses per carport
N_{TypCS}	3	series rigid buses carport
	1	series articulated buses carport
N_{TypCP}	1	parallel rigid buses carport
	5	parallel articulated buses carport
$N_{i\prime}^{s\mathrm{THV}}$	1 x 25 MVA 110/20 kV	transformers
P_{THV}	25	MVA
P_{Typ}	2	MVA for rigid buses transformer
	2	MVA for articulated buses transformer
N_{TVTyp}	3 x 2 MVA 20/0.4 kV	rigid buses transformers
	5 x 2 MVA 20/0.4 kV	articulated buses transformers
N_{ij}^{cHV}	1516 m x N2XSH 1 x 500/35 20kV	cables
N_{ij}^{cTyp}	1536 m x NSGAFÖU 4 x (4 x 1 x 300 mm²) 0.4 kV	cables
	3080 m x NSGAFÖU 4 x (4 x 1 x 300 mm²) 0.4 kV	cables
N_{ij}^{cCH}	4720 m x NYCWY 4 x 120/70 0.4 kV	cables
V_{SHV}	20	kV
C_{Total}	3,008,136	€
L_{TSC}	195	m
W_{TPC}	108	m

E. IN CASE OF VARYING THE CHARGING POWER

As indicated previously in TABLE 1, the charging power (P_{Ch}) for each bus is defined as a constant equal to 150 kW in

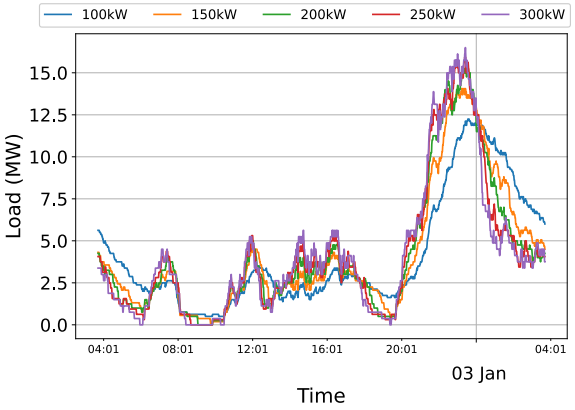

FIGURE 14. Load profiles of the modelled bus depot, where the total load is calculated considering various charging power levels over the period of 24 h.

TABLE 8. Effect of various charging power levels on the chosen components for the power system and the system total cost.

P_{Ch}	100 kW	150 kW	200 kW	250 kW	300 kW
1.25 · (P_N)	12.25 MVA	14.06 MVA	15.25 MVA	15.94 MVA	16.5 MVA
$N_{ii'}^{STHV}$	-	1 x 25 MVA 110/20 kV	1 x 25 MVA 110/20 kV	1 x 25 MVA 110/20 kV	1 x 25 MVA 110/20 kV
N_{TVTyp} (rigid buses)	3 x 2 MVA 10/0.4 kV	3 x 2 MVA 20/0.4 kV	4 x 1.6 MVA 20/0.4 kV	4 x 2 MVA 20/0.4 kV	4 x 2 MVA 20/0.4 kV
N_{TVTyp} (Articulated buses)	4 x 2 MVA 10/0.4 kV	5 x 2 MVA 20/0.4 kV	5 x 2 MVA 20/0.4 kV	5 x 2 MVA 20/0.4 kV	5 x 2 MVA 20/0.4 kV
C_{Total} (k€)	2,204	2,909	3,022	3,089	3,089

the previous cases. In this sensitivity case, various charging power levels are implemented to observe their effects on the load profile and, consequently, on the design of the power system. As shown in FIGURE 14, this results in different power peaks and times of occurrence. As the charging power increases, buses require less charging time. This results in a relatively flattened curve when charging at 100 kW compared with that at 300 kW.

As shown in TABLE 8, changing the charging power of the buses significantly affects the design of the power system.

Starting by applying 100 kW charging power, the MIQP model chose the connection of the bus depot directly to a 10 kV-grid. This has the advantage of being less expensive, but has the disadvantage of having to charge buses all the time. Consequently, this could force the system to its limits, particularly in the case of charger failure. Additionally, current developments in the field of electric vehicles aim to charge at higher power levels to benefit from fast-charging technology. However, having a connection to the 110 kV-grid enabled several charging power levels, without having to extend the medium-voltage network. The observed differences between various charging powers emphasize the need to install additional distribution transformers in the carports as of increasing the charging power. This is accompanied by the need to connect more cables and incurs higher costs.

V. CONCLUSION

This study proposes a MIQP model for the charging infrastructure of electric bus depots. Using this model, it is possible to determine the dependencies of each component on others. One of the drawbacks of the MIQP model is the high computation time required. This owes to the fact, that the problem must be explicitly defined through constraints, which are connected to each other technically and economically. The advantages of the MIQP model are summarized in two main points. On one side, it is capable of solving optimization problems with high degree of complexity, where the relation between constraints is non-linear. On the other side, it is possible after defining the constraints to generate an optimum model based on the available few input data, which is usually the case in the early stages of the designing process. This is realized by considering the system as a group of blocks that vary in their number and parameters. Initially, different types of transformers and cables are integrated into the model. The conclusive parameter in this design process is the load profile, which is calculated based on the planned routes served by the depot. Given that these routes can change over time, an additional 25% loading is considered in the model to extend the eligibility of the depot for higher consumption. This causes the peak load to exceed 14 MW, which requires a connection to a 110 kV-grid. Based on this fact, the model starts to build the power circuit by choosing the optimum transformers and cables until a 0.4 kV-grid is reached.

Simultaneously, some sensitivity studies are conducted using this model to demonstrate various possible designs with different objectives. By implementing the case of having the least available area, all buses could fit into only two carports in the form of one carport per each type of buses. The objective of this case study is to reach a design, that guarantees optimum usage for an area at the lowest cost. In the second case, an additional constraint is considered to limit the available area of the carports and enable the implementation of simpler firefighting precautions in the depot. This approach results in an increase in the number of carports. Whereas in the third case, these precautions are extended by additional limitations of number of buses per carport. This results in an increase in the number of carports, that leads to the increase in cable lengths and the system total costs consequently. In the fourth case, the blocking of buses to each other is intentionally limited. This caused an increase in the occupied area of the depot along with an increase in the system total cost. It also showed the limits of the available area. The above-mentioned sensitivity case studies (A-D) show a variety of possible configurations to serve the planned routes. This model enables bus operators to

choose their main objectives, knowing their effects on other system components. For instance, if a bus operator focuses on reducing the occupied area, cases A and C would be relevant. However, they lead to minimum number of carports, which is challenging for firefighting precautions. In the fifth case, the effect of varying the charging power on the charging infrastructure is observed, demonstrating the ability of the components to support higher charging powers. Finally, the model shows a compromise between the required number of buses, available area, required components for the system, and their effect on the total cost. This model can be used in the early planning phases of bus depots to investigate the feasibility of serving the targeted routes. However, in future research, we plan to consider the effect of bus distribution among parking spaces to achieve the lowest blocking probability by implementing various utility factors and charging capacities for the chargers. In addition, the redundancy of the components in the failure cases is to be calculated based on the loading of each component. Additionally, the weather was assumed to be always −15 °C to consider the maximum required pre-heating for the buses, which will vary in future research work.

ACKNOWLEDGMENT

The authors thank HOCHBAHN AG and Verkehrsbetriebe Hamburg-Holstein GmbH (VHH) for their cooperation and support.

REFERENCES

[1] GFE Agency. (Feb. 7, 2022). *Handbuch Für Emissionsfaktoren (HBEFA)*. Accessed: Feb. 14, 2022. [Online]. Available: https://www.umweltbundesamt.de/themen/verkehr-laerm/emissionsdaten#hbefa

[2] M. Rogge, E. Van Der Hurk, A. Larsen, and D. U. Sauer, "Electric bus fleet size and mix problem with optimization of charging infrastructure," *Appl. Energy*, vol. 211, pp. 282–295, Feb. 2018.

[3] D. Jefferies and D. Göhlich, "A comprehensive TCO evaluation method for electric bus systems based on discrete-event simulation including bus scheduling and charging infrastructure optimisation," *World Electric Vehicle J.*, vol. 11, no. 3, p. 56, Aug. 2020.

[4] A. Kunith, R. Mendelevitch, and D. Goehlich, "Electrification of a city bus network: An optimization model for cost-effective placing of charging infrastructure and battery sizing of fast charging electric bus systems," *Int. J. Sustain. Transp.*, vol. 11, no. 11, pp. 707–720, 2017.

[5] L. Haffner, M. Schumann, D. Schulz, and M. Dietmannsberger, "Evaluation of modular infrastructure concepts for large-scaled electric bus depots," in *Proc. 2nd E-Mobility Power Syst. Integr. Symp.*, Stockholm, Sweden, 2018.

[6] N. A. El-Taweel, H. E. Z. Farag, G. Barai, H. Zeineldin, A. Al-Durra, and E. F. El-Saadany, "A systematic approach for design and analysis of electrified public bus transit fleets," *IEEE Syst. J.*, vol. 16, no. 2, pp. 2989–3000, Jun. 2022.

[7] E. Lauth, P. Mundt, and D. Gohlich, "Simulation-based planning of depots for electric bus fleets considering operations and charging management," in *Proc. 4th Int. Conf. Intell. Transp. Eng. (ICITE)*, Singapore, Sep. 2019, pp. 327–333.

[8] H. Basma, M. Haddad, C. Mansour, M. Nemer, and P. Stabat, "Assessing the charging load of battery electric bus fleet for different types of charging infrastructure," in *Proc. IEEE Transp. Electrific. Conf. Expo (ITEC)*, Chicago, Illinois, Jun. 2021, pp. 887–892.

[9] J. Chen, B. Atasoy, T. Robenek, M. Bierlaire, and M. Themans, "Planning of feeding station installment for electric urban public mass-transportation system," in *Proc. 13th Swiss Transp. Res. Conf.*, Ascona, Switzerland, 2013, pp. 1–15.

[10] O. Beaude, S. Lasaulce, M. Hennebel, and I. Mohand-Kaci, "Reducing the impact of EV charging operations on the distribution network," *IEEE Trans. Smart Grid*, vol. 7, no. 6, pp. 2666–2679, Nov. 2016.

[11] G. Piazza, S. Bracco, F. Delfino, and S. Siri, "Optimal design of electric mobility services for a local energy community," *Sustain. Energy, Grids Netw.*, vol. 26, Jun. 2021, Art. no. 100440.

[12] A. Fathollahi, S. Y. Derakhshandeh, A. Ghiasian, and M. H. Khooban, "Utilization of dynamic wireless power transfer technology in multi-depot, multi-product delivery supply chain," *Sustain. Energy, Grids Netw.*, vol. 32, Dec. 2022, Art. no. 100836.

[13] S. Bracco, G. Dentici, and S. Siri, "DESOD: A mathematical programming tool to optimally design a distributed energy system," *Energy*, vol. 100, pp. 298–309, Apr. 2016.

[14] S. N. Gowda, A. Ahmadian, V. Anantharaman, C.-C. Chu, and R. Gadh, "Power management via integration of battery energy storage systems with electric bus charging," in *Proc. IEEE Power Energy Soc. Innov. Smart Grid Technol. Conf. (ISGT)*, Apr. 2022, pp. 1–5.

[15] C. Yao, S. Chen, and Z. Yang, "Joint routing and charging problem of multiple electric vehicles: A fast optimization algorithm," *IEEE Trans. Intell. Transp. Syst.*, vol. 23, no. 7, pp. 8184–8193, Jul. 2022.

[16] P. K. Saha, N. Chakraborty, A. Mondal, and S. Mondal, "Optimal sizing and efficient routing of electric vehicles for a vehicle-on-demand system," *IEEE Trans. Ind. Informat.*, vol. 18, no. 3, pp. 1489–1499, Mar. 2022.

[17] M. A. Mejia, L. H. Macedo, G. Munoz-Delgado, J. Contreras, and A. Padilha-Feltrin, "Multistage planning model for active distribution systems and electric vehicle charging stations considering voltage-dependent load behavior," *IEEE Trans. Smart Grid*, vol. 13, no. 2, pp. 1383–1397, Mar. 2022.

[18] A. Almunif and L. Fan, "Mixed integer linear programming and nonlinear programming for optimal PMU placement," in *Proc. North Amer. Power Symp. (NAPS)*, Sep. 2017, pp. 1–6.

[19] J. Hinker, T. Wohlfahrt, E. Drewing, S. C. Paredes, D. M. González, and J. Myrzik, "Adaptable energy systems integration by modular, standardized and scalable system architectures: Necessities and prospects of any time transition," *Energies*, vol. 11, no. 3, p. 581, Mar. 2018.

[20] P. C. Paiva, H. M. Khodr, J. A. Dominguez-Navarro, J. M. Yusta, and A. J. Urdaneta, "Integral planning of primary-secondary distribution systems using mixed integer linear programming," *IEEE Trans. Power Syst.*, vol. 2, no. 20, pp. 1134–1143, May 2005.

[21] M. Eskander, A. Jahic, and D. Schulz, "Reliability analysis of large-scale electric bus depots based on different failure scenarios," in *Proc. IEEE Electric Power Energy Conf. (EPEC)*, Edmonton, AB, Canada, Nov. 2020, pp. 1–6.

[22] L. Thurner, A. Scheidler, F. Schafer, J.-H. Menke, J. Dollichon, F. Meier, S. Meinecke, and M. Braun, "Pandapower—An open-source Python tool for convenient modeling, analysis, and optimization of electric power systems," *IEEE Trans. Power Syst.*, vol. 33, no. 6, pp. 6510–6521, Nov. 2018.

[23] T. Brown, J. Hörsch, and D. Schlachtberger, "PyPSA: Python for power system analysis," *J. Open Res. Softw.*, vol. 6, no. 1, p. 4, Jan. 2018.

[24] R. C. Dugan and T. E. McDermott, "An open source platform for collaborating on smart grid research," in *Proc. IEEE Power Energy Soc. Gen. Meeting*, Detroit, MI, USA, Jul. 2011, pp. 1–7.

[25] M. Eskander, A. Jahic, D. Schulz, T. Muller, N. Zeun, and O. Hoffmann, "Aufbau und optimierung von ladeinfrastrukturen auf busbetriebshofen (in English: Design and optimization of charging infrastructure of bus depots)," in *Hamburger Beitrage Zum Technischen Klimaschutz*. Hamburg, Germany: Helmut-Schmidt-Universitat/Universitat der Bundeswehr, 2021, pp. 153–159.

[26] S. Liang, M. Ma, and S. He, "Multiobjective optimal formulations for bus fleet size of public transit under headway-based holding control," *J. Adv. Transp.*, vol. 2019, pp. 1–14, Jan. 2019.

[27] A. Jahic, M. Eskander, and D. Schulz, "Charging schedule for load peak minimization on large-scale electric bus depots," *Appl. Sci.*, vol. 9, no. 9, p. 1748, Apr. 2019.

[28] M. Blumstengel, R. Herms, S. Kamender, H. Kähler, T. Krämer, M. Sievers, and J. Schmitz, "Richtlinie für den von omnibus-busbetriebshofen (in English: Guideline for bus depots) VDV-schrift 822," Verband Deutscher Verkehrsunternehmen e. V. (VDV), Cologne, Germany, Tech. Rep. 822, 2016.

[29] H. Kiank and W. Fruth, *Planning Guide for Power Distribution Plants: Design, Implementation and Operation of Industrial Networks*. Germany: H. Kiank and W. Fruth, 2012.
[30] H. Klaus, K.-D. Dettmann, and D. Schulz, *Elektrische Energieversorgung* (Electrical Energy Generation). Wiesbaden, Germany: Springer, 2013.
[31] *Nach Großbrand in Hamburg—Forderungen Nach Mehr Brandschutz Für E-Bus-Betriebshöfe*, Welt.de, 2021.

MINA ESKANDER received the B.Sc. degree in electrical power engineering from Ain Shams University, Cairo, Egypt, in 2013, and the M.Sc. degree in electrical engineering from the Karlsruhe University of Applied Sciences, Karlsruhe, Germany, in 2017. He is currently a Research Assistant with the Institute of Electrical Power Systems, Helmut Schmidt University/University of the Bundeswehr Hamburg, Hamburg, Germany. His current research interests include planning of charging infrastructure for electromobility, optimization of power systems, applications of machine learning in electrical power systems, design of smart grids, and optimal integration of renewable energy sources in power systems.

MAIK PLENZ received the M.Eng. degree in business administration and engineering/energy management from the Technical University of Cottbus–Senftenberg, UAS Senftenberg, Germany, in 2012. He was a Research Assistant with the Technical University of Cottbus–Senftenberg and the Leuphana University of Lüneburg. He is currently a Research Assistant with the Institute of Electrical Power Systems, Helmut Schmidt University/University of the Bundeswehr Hamburg, Hamburg, Germany. His research interests include distribution grids, simulation, and optimization of electrical grids, energy management/storage, e-mobility and digitization, and data science in general, which are pursued at the DLab—Distributed Energy Laboratory.

EDVARD AVDEVICIUS received the B.Sc. degree in mechatronics and robotics from Vilnius Gediminas Technical University, Vilnius, Lithuania, in 2017, and the M.Sc. degree in mechatronics from the Hamburg University of Technology, Hamburg, Germany, in 2022. He is currently a Research Assistant with the Institute of Electrical Power Systems, Helmut Schmidt University/University of the Bundeswehr Hamburg, Hamburg. His research interest includes the development of smart grids and electric mobility projects using process optimization, building automation techniques, and control theory.

DETLEF SCHULZ (Senior Member, IEEE) received the Dipl.-Ing. degree in electrical engineering from the Technical University of Cottbus, Germany, in 1997, and the Dr.-Ing. and Venia Legendi degree in electrical engineering from the Technical University of Berlin, Berlin, Germany, in 2002 and 2006, respectively. From 1997 to 1999, he was with ABB Industrial Automation, Cottbus, Germany. Since 2006, he has been a Full Professor and the Head of the Institute of Electrical Power Systems, Helmut Schmidt University/University of the Bundeswehr Hamburg, Hamburg, Germany. His research interests include electrical power systems and on-board electrical systems: grid integration and grid conformity of distributed generation and electromobility, grid impedance measurement, grid protection, and internal electrical control of fuel cells, which are pursued at the DLab—Distributed Energy Laboratory. He is a member of the VDE ETG and IEEE PES and a Full Member of the Academy of Sciences and Humanities, Hamburg.